Recognizing the role of Tropical Seaways in modulating the Pacific circulation

N. Tan, Z. Zhang, Z. Guo, C. Guo, Z. Zhang, Z. He, G. Ramstein

Geophysical Research Letters

RESEARCH LETTER
10.1029/2022GL099674

Recognizing the Role of Tropical Seaways in Modulating the Pacific Circulation

N. Tan[1,2], Z. S. Zhang[3,4], Z. T. Guo[1,5,6], C. C. Guo[7], Z. J. Zhang[1,2], Z. L. He[1,2], and G. Ramstein[8]

[1]Key Laboratory of Cenozoic Geology and Environment, Institute of Geology and Geophysics, Chinese Academy of Sciences, Beijing, China, [2]Innovation Academy for Earth Science, Chinese Academy of Sciences, Beijing, China, [3]Department of Atmospheric Science, School of Environmental Studies, China University of Geosciences, Wuhan, China, [4]Nansen-Zhu International Research Centre, Institute of Atmospheric Physics, Chinese Academy of Sciences, Beijing, China, [5]CAS Center for Excellence in Life and Paleoenvironment, Beijing, China, [6]University of Chinese Academy of Sciences, Beijing, China, [7]NORCE Norwegian Research Centre, Bjerknes Centre for Climate Research, Bergen, Norway, [8]Laboratoire des Sciences du Climat et de l'Environnement, LSCE/IPSL, CEA-CNRS-UVSQ, Université Paris-Saclay, Gif-sur-Yvette, France

Abstract Various modeling studies have examined the climatic effects of either the Central American Seaway or the Indonesian seaway. The co-existence of these two tropical seaways may have a greater influence than the existence of a single seaway. Although the dual seaway situation is closer to that reconstructed during Miocene/Pliocene, relevant studies remain scarce. Here, we investigate the co-effects of dual tropical seaway changes on the Pacific circulation through a set of sensitivity experiments. Our results show that the combined shallow opening of tropical seaways can generate an active Pacific meridional overturning circulation and maintain strong upwelling conditions along the equatorial Pacific, which may have helped favor a "biogenic bloom" during the late Miocene and early Pliocene. Moreover, the logically successive closure of the tropical seaways can provide patterns of zonal sea surface temperature gradients that are similar to those recorded in the equatorial Pacific from the late Miocene to the Pliocene.

Plain Language Summary During the late Miocene and the Pliocene, changes in the Central American and the Indonesian seaways geometry are very important for ocean circulation and global climate. Various modelling studies have examined the separate effects of these two tropical seaways, especially their link to the onset of the Northern Hemisphere ice sheets through changes in the Atlantic meridional overturning circulation and associated heat and moisture transport. Although the existence of dual tropical seaways is closer to the reality, there are very scarce modelling studies exploring the co-effects of dual tropical seaway changes, especially on the Pacific ocean circulation. Here we provide the results of modelling study on this issue. Our results show that the combined shallow opening of tropical ways can generate an active Pacific meridional overturning circulation (i.e., absent in modern conditions) by which the meridional and zonal sea surface temperature gradient in the Pacific largely reduce. In contrast, a deeper opening of tropical seaways can not produce these changes in the Pacific ocean circulation. This study provides insights into and a better understanding of the role of tropical seaways in shaping the Pacific climate and highlights the importance of the sill depth of each seaway.

Key Points:

- The co-effects of opening of two tropical seaways on the Pacific circulation are investigated with climate model
- Shallow opening of tropical seaways can generate an active Pacific meridional overturning circulation, whilst a deeper condition can not
- The stepwise closure of the tropical seaways can provide similar-to-record patterns of zonal sea surface temperature gradients

Supporting Information:

Supporting Information may be found in the online version of this article.

Correspondence to:

N. Tan,
ning.tan@mail.iggcas.ac.cn

Citation:

Tan, N., Zhang, Z. S., Guo, Z. T., Guo, C. C., Zhang, Z. J., He, Z. L., & Ramstein, G. (2022). Recognizing the role of tropical seaways in modulating the Pacific circulation. *Geophysical Research Letters*, *49*, e2022GL099674. https://doi.org/10.1029/2022GL099674

Received 23 MAY 2022
Accepted 27 SEP 2022

Author Contributions:

Conceptualization: N. Tan, Z. S. Zhang
Formal analysis: N. Tan
Funding acquisition: Z. T. Guo
Investigation: N. Tan
Methodology: N. Tan, Z. S. Zhang, C. C. Guo
Project Administration: Z. T. Guo
Supervision: Z. S. Zhang, Z. T. Guo, G. Ramstein
Validation: N. Tan, C. C. Guo
Writing – original draft: N. Tan
Writing – review & editing: N. Tan, Z. S. Zhang, Z. T. Guo, C. C. Guo, Z. J. Zhang, Z. L. He, G. Ramstein

1. Introduction

From the late Miocene to the Pliocene, enormous changes occurred in the Earth's climate and ecosystems, such as a sustained global cooling in the ocean (Herbert et al., 2016), the global expansion of C4 grasses (Cerling et al., 1997; Huang et al., 2007), high biogenic activities at numerous locations (Drury et al., 2021; Farrell et al., 1995; Karatsolis et al., 2022; Schroeder et al., 1997), and the onset of Northern Hemisphere ice sheets (Jansen & Sjøholm, 1991; Maslin et al., 1998). In this period, changes in tropical seaways-the Central American Seaway (CAS) and Indonesian seaway-had reached their critical threshold and may have triggered fundamental changes in regional or global climate (e.g., Cane & Molnar, 2001; Driscoll & Haug, 1998). However, the evidence for these gateway changes is complex and sometimes controversial. The results of detrital zircon U-Pb geochronology carried out on samples from the northern Andes indicate the CAS had vanished with the last fluvial connection in the middle Miocene (Montes et al., 2015). In contrast, various geochemical, paleontological,

and molecular marine records have suggested that the CAS was not fully closed until the late Pliocene (See the synthesis in O'Dea et al., 2016, and references therein). During the late Miocene, the water connection through the CAS may have existed at subsurface to intermediate depths (200–500 m) (Coates & Stallard, 2013). Further shoaling of CAS between 4.8 and 4.2 Ma may lead to water exchanges constrained above ~200 m (Haug et al., 2001). Since early Cenozoic, the Australia plate had been moving slowly towards the equator and gradually converging with Sundaland plate. This process was accompanied by the disappearance of some volcanic arcs as well as emergence of new chain islands around this region, thus forming the narrow and complex channel (known as Indonesian seaway) connecting the Pacific and Indian Ocean (Hall, 2002). The modern configuration of the Indonesian seaway is thought to date from around 4–3 Ma (Auer et al., 2019; Gaina & Müller, 2007; Hall, 2002), though more detailed picture of Indonesian seaway evolution is not available.

Numerous modeling studies have investigated the individual impacts of the CAS and Indonesian seaway on the regional and global climates. Previous studies have revealed that the closure of the CAS strengthens the the Atlantic meridional overturning circulation (AMOC) and alters heat and moisture transport and thus might contribute to the onset of Northern Hemisphere ice sheets (Brierley & Fedorov, 2016; Keigwin, 1982; Lunt et al., 2008). The Indonesian seaway constriction may alter the exchange of water between the Pacific and Indian oceans (Jochum et al., 2009; Rodgers et al., 2000) and cause sub-surface cooling in the Indian Ocean (Karas et al., 2009) and aridification in both Australia (Christensen et al., 2017; Krebs et al., 2011) and East Africa (Cane & Molnar, 2001). However, many modeling studies have suggested that the impact of the changes in the Indonesian seaway on global climate was weak in the Miocene/Pliocene (Brierley & Fedorov, 2016; Fedorov et al., 2013; Jochum et al., 2009).

Few modeling studies have considered the co-effect of CAS closing and Indonesian seaway constriction, despite the associated change of the two gateways being likely across the Miocene and Pliocene. Song et al. (2017) studied the relative contribution of deep opening of the CAS (1,200 m) and a widened Indonesian seaway on El Niño-Southern oscillation (ENSO) amplitudes and variability. However, there still lacks studies of the impact of shallow opening of both tropical seaways, which might correspond to the conditions at the Miocene-Pliocene boundary. Meanwhile, North Pacific Deep Water (NPDW) and the Pacific meridional overturning circulation (PMOC) may be active and associated with the greatly reduced meridional Pacific sea surface temperature (SST) gradient during the late Miocene-Pliocene, as evidenced by geological records and modeling results (Burls et al., 2017; Ford et al., 2022; Thomas et al., 2021). A recent study by Shankle et al. (2021) has associated the occurrence of the "biogenic bloom" in the Eastern Equatorial Pacific (EEP) at the Miocene-Pliocene boundary (Farrell et al., 1995; Schroeder et al., 1997) with this active PMOC. Under modern conditions, the PMOC and NPDW are absent; this is attributed to the extra fresh water input (P–E) in the subarctic Pacific that stratifies the upper ocean (Ferreira et al., 2018).

Because the water transported through the CAS and Indonesian seaway is from the Pacific, the co-existence of the CAS and Indonesian seaway may have led to fundamental changes in the Pacific ocean circulation and air-sea interactions around the Miocene-Pliocene boundary. Thus, further investigation of the co-existence of the CAS and Indonesian seaway will allow a more comprehensive understanding of their role in climatic changes at this time. In this study, based on a set of seaways sensitivity experiments with the low-resolution version of the Norwegian Earth System Model (NorESM-L; Z. S. Zhang et al., 2012), we aim to investigate the impact of the co-occurrence of the CAS and Indonesian seaway on Pacific circulation, including deep water formation and the Equatorial upwelling system. We also discuss the potential role of these two tropical seaways in shaping the zonal/meridional SST gradients and "biogenic bloom" that occurred in the late Miocene-early Pliocene.

2. Method

2.1. Climate Model

The NorESM is based on the structure of the Community Earth System Model (CESM) from the National Center for Atmospheric Research (NCAR), but with a new ocean component that originated from the Miami Isopycnic Coordinate Ocean Model (MICOM; Bleck et al., 1992). The NorESM-L is designed specifically for paleoclimate studies. The resolution of the atmosphere component (the spectral Community Atmosphere Model CAM4; Neale et al., 2013) is T31 (~3.75°) in the horizontal and 26 levels in the vertical. The resolution of the ocean component is g37 (~3°) in the horizontal and 32 layers in the vertical. Additional details of the model can be found in Bentsen

et al. (2013) and Z. S. Zhang et al. (2012). The NorESM-L has shown good performance in the pre-industrial simulation (Z. S. Zhang et al., 2012), and it has contributed to the Pliocene Model Inter-comparison Project Phase 1 (PlioMIP 1; Z. S. Zhang et al., 2012) and Phase 2 (PlioMIP2; Li et al., 2020). This model can simulate a reasonable modern AMOC but with stronger magnitude (21.8 Sv, Z. S. Zhang et al., 2012) than the observations (17.2 Sv, McCarthy et al., 2015). Despite the coarse oceanic resolution and the lack of presence of small islands around the Indonesian seaway, the NorESM-L modeled annual mean total Indonesian throughflow (ITF) is about 14.1 Sv (1 Sv = 10^6 m^3/s) in the pre-industrial experiment, which is within the range of modern mooring-based observations (10.7–18.7 Sv; Sprintall et al., 2009).

2.2. Experimental Design

To investigate the impact of tropical seaways and the contribution of each individual seaway, we designed eight experiments in this study; that is, one control and seven sensitivity experiments. The PlioMIP 2 core experiment run with the NorESM-L (Li et al., 2020) is used as the control experiment, hereafter referred to as "Plio_ctrl." The boundary conditions of Plio_ctrl are adapted from the Pliocene Research, Interpretation, and Synoptic Mapping version 4 (PRISM4; Dowsett et al., 2016). Starting from the equilibrium state of Plio_ctrl, we carried out seven other experiments. The boundary conditions of these experiments are identical to Plio_ctrl, except for the modification in the tropical seaways (Figures 1a–1d). First, we widened the Indonesian seaway and opened the CAS by setting two different sill depths for the new ocean grids (100 and 500 m, hereafter referred to as "IndoCAS100" and "IndoCAS500"). As shown in Figures 1b and 1d, the Indonesian seaway in IndoCAS100/500 has been enlarged by removing the land grid points over northern New Guinea and the central-eastern part of Java island. Due to the coarse resolution in our model, some micro islands located around Makassar Strait are not present in the model grid. The opening CAS is located in the Panama region with three model land grid points removed. Furthermore, we designed another experiment ("IndoCAS100_half," Figure 1c) to depict a narrow open state of tropical seaways, with half the width of the Indonesian seaway and CAS relative to IndoCAS100. Finally, we designed four single seaway experiments to distinguish the relative effects of the Indonesian seaway and CAS. They are the Indonesian seaway-only (Indo100 and Indo500) and CAS-only (CAS100 and CAS500) experiments with depths of 100 and 500 m for the new ocean grids. The single seaway settings in these four experiments are the same as the corresponding open seaway conditions in IndoCAS100 or IndoCAS500. Note that we modified these two tropical seaways broadly following the available reconstruction of the period between the late Miocene and the early Pliocene (Hall, 2002; Molnar & Cronin, 2015), though some details are not included because of the coarse resolution of the model and the large uncertainty in the reconstruction.

We integrated all of the experiments for 1,600 years and analyzed the last 100-year outputs. The Plio_ctrl experiment is also extended for 1,600 years to give the same integration period. A summary of the experimental configurations is listed in Table S1 in Supporting Information S1. Analyses in the Results and Discussion sections are all calculated on the basis of mean annual values.

3. Results

3.1. Water Flux Through Tropical Seaways and Circulation Change

In our simulations, the net water transport through the Indonesian seaway are mostly southward except for CAS500 (see values in Table S2 in Supporting Information S1), while the water transport varies considerably at different depths in each experiment (Figures 1e and 1f). Experiments without opening CAS (Plio_ctrl, Indo100, and Indo500) and experiment of IndoCAS100_half show nearly consistent southward water transport (from the Pacific to the Indian Ocean) above ~1,300 m through the Indonesian seaway (Figure 1e). However, in the cases with opening CAS (except for IndoCAS100_half), the water transport turns to northward at the depth ranging from ~180–200 m to ~400–600 m. With deeper opening CAS (IndoCAS500 and CAS500), more water transports from Indian Ocean to the Pacific at the depth of ~200–600 m. This is consistent with the water transport through the CAS (Figure 1f), which show more water flowing from the Pacific to the Atlantic in deeper opening CAS cases. The water transport through CAS is uniformly eastward and likely related with the width and depth of the CAS, whereas the water mass transport through the Indonesian seaway are more complex. The opening of CAS is important to influence the net water transport through the Indonesian seaway.

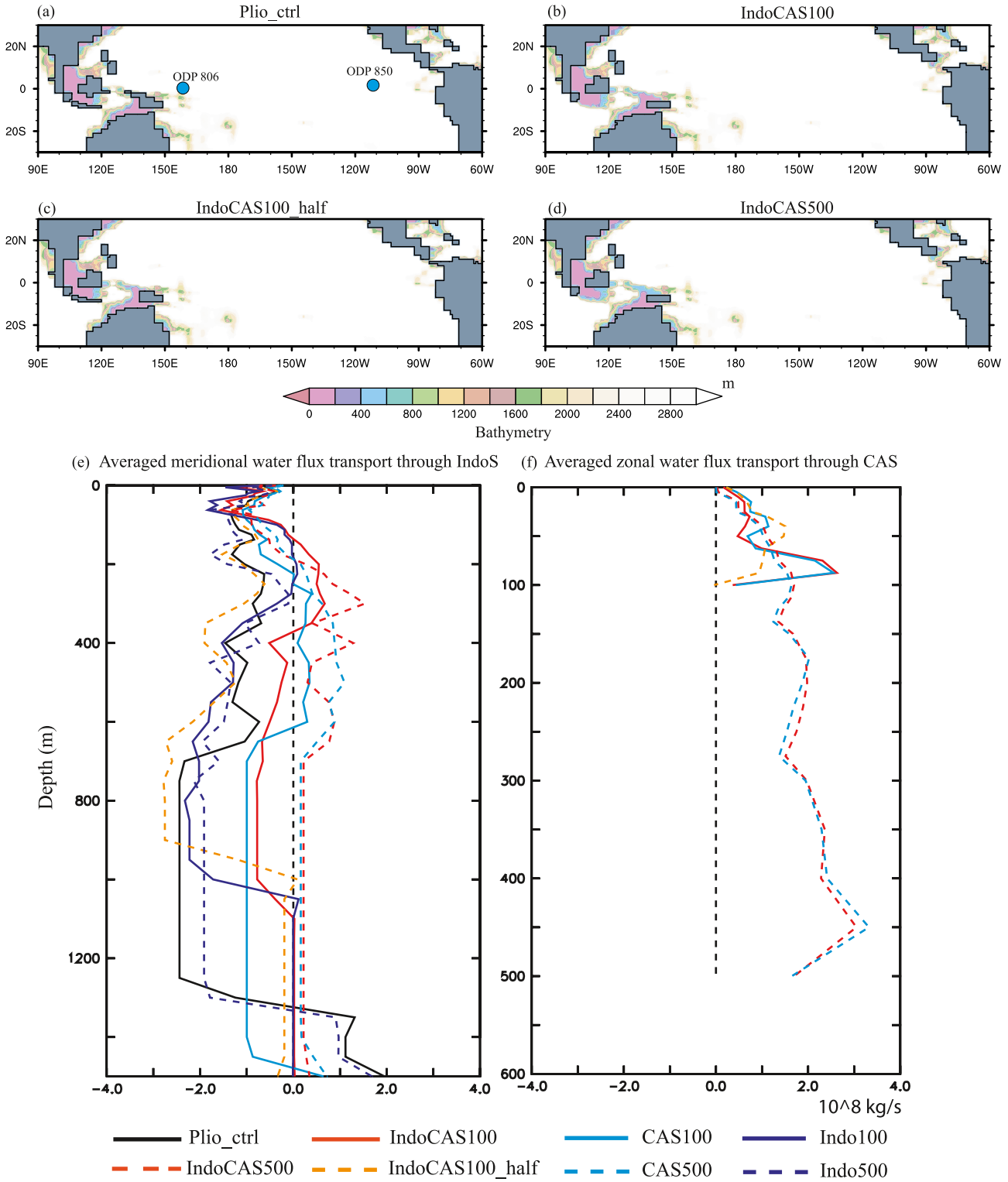

Figure 1. Land mask and bathymetry over tropical Pacific for each experiment (a–d), blue circles represent the locations of ocean drilling project 806 and 850, (e) meridional water mass transport through Indonesian seaway, and (f) zonal water mass transport through Central American Seaway. The positive values in water mass transport (e and f) indicate respectively northward and eastward water transport.

The barotropic stream function (defined as the depth-integrated zonal water volume transport and in which the positive values indicate clockwise flow) show that the opening tropical seaways can generally weaken the subtropical gyres and north equatorial current system and enhance the Equatorial countercurrent in comparison with Plio_ctrl (Figure S2 in Supporting Information S1). More specifically, IndoCAS100 and IndoCAS100_half show relatively stronger northward current along the West boundary; IndoCAS500 presents significant weakening in the South Pacific subtropical gyre and shows large enhancement of equatorial countercurrent. IndoCAS100_half allows more sea water bypassing southern New Guinea toward Indonesian seaway (Figure S2d in Supporting Information S1) comparing to Plio_ctrl. This may explain the larger transport of seawater to the Indian Ocean in IndoCAS100_half.

3.2. PMOC Formation

In Plio_ctrl, the simulated North Pacific Intermediate Water is a modern-like state with a strength of 4.9 Sv above 1,000 m (Figure 2a and Table S2 in Supporting Information S1). In contrast, the PMOC becomes active when the two tropical seaways are open and shallow (IndoCAS100 and IndoCAS100_half, Figures 2b and 2d). More specifically, the PMOC is deeper and stronger (1,800–2,000 m, 16.0 Sv) in IndoCAS100 than that in IndoCAS100_half (1,000–1,200 m, 12.3 Sv). However, when the tropical seaways are deeper (IndoCAS500, Figure 2c), the PMOC disappears.

By comparing with the single seaway experiments (Figures 2e–2h), we find that the formation of PMOC is primarily due to the shallow opening Indonesian seaway (Indo100, Figure 2e), while Indo500 and CAS100/500 cannot promote the formation of the meridional overturning circulation over North Pacific (Figures 2f–2h). We further find that in active-PMOC cases (IndoCAS100, IndoCAS100_half, and Indo100), the salinities over subarctic Pacific region (Figure S3 in Supporting Information S1) are larger than those in inactive-PMOC cases (Plio2, IndoCAS500, CAS100, CAS500, and Indo500). Thus, this denser water in IndoCAS100, IndoCAS100_half, and Indo100 over subarctic Pacific region helps weaken the upper ocean stratification and promote the formation of the deep water. The differences in salinity changes between these two cases (active-PMOC and inactive-PMOC) are found to be highly related with the net precipitation (calculated with mean annual precipitation minus evaporation and plus runoff) over subarctic Pacific region (Figure 2i), showing lower net precipitation and higher salinity. These results may reflect that the salinity changes over subarctic Pacific regions linking to the net precipitation are important for the state of the PMOC. Logically, with active PMOC (IndoCAS100, IndoCAS100_half, and Indo100), more ocean heat is transported towards high latitudes (Figure S4 in Supporting Information S1) hence leading to decreasing of meridional SST gradients in the North Pacific in these experiments (Table S2 in Supporting Information S1 and Figure 2j). In turn, the decreased meridional SST gradients may further result in a positive feedback to sustain the active PMOC, which has been demonstrated by recent works by Burls et al. (2017) and Ford et al. (2022).

3.3. Equatorial Upwelling Strength

The opening of tropical seaways also leads to responses in the Equatorial upwelling system. Here, we define the total upwelling strength as the maximum value of horizontally integrated vertical water flux (3°S–3°N, 170–95°W) above the depth of 400 m. The upwelling strengths along 170–95°W are presented in Figure 3. It should be pointed out that due to the relatively coarse resolution of this model, physical process related to the coastal ocean are not well presented. Thus, the simulated strongest upwelling here are located near the Central Equatorial Pacific (CEP) instead of the EEP. In total, the shallow opening tropical seaways (IndoCAS100) can generate stronger upwelling in comparison with other experiments (Figure 3a and Table S2 in Supporting Information S1). This is mainly due to the obvious intensification of upwelling over west of 140°W in IndoCAS100, which is beyond the magnitude of decreasing of upwelling over east of 140°W. The single seaway experiments further reveal that the shallow opening of CAS (CAS100) acts to intensify the upwelling in the EEP, while the shallow opening of Indonesian seaway reduces the upwelling in the EEP but intensifies the upwelling in the CEP (Figure 3b). The single deep CAS (CAS500) or Indonesian seaway (Indo500) has very similar effects on the upwelling to the combined situation (IndoCAS500), which is similar with the condition of Plio_ctrl (Figure 3c).

The Equatorial upwelling strength is closely linked to the easterly wind that generates Ekman pumping (Kessler, 2006). In our model, modern-like northeast and southeast wind stress are simulated along the equatorial

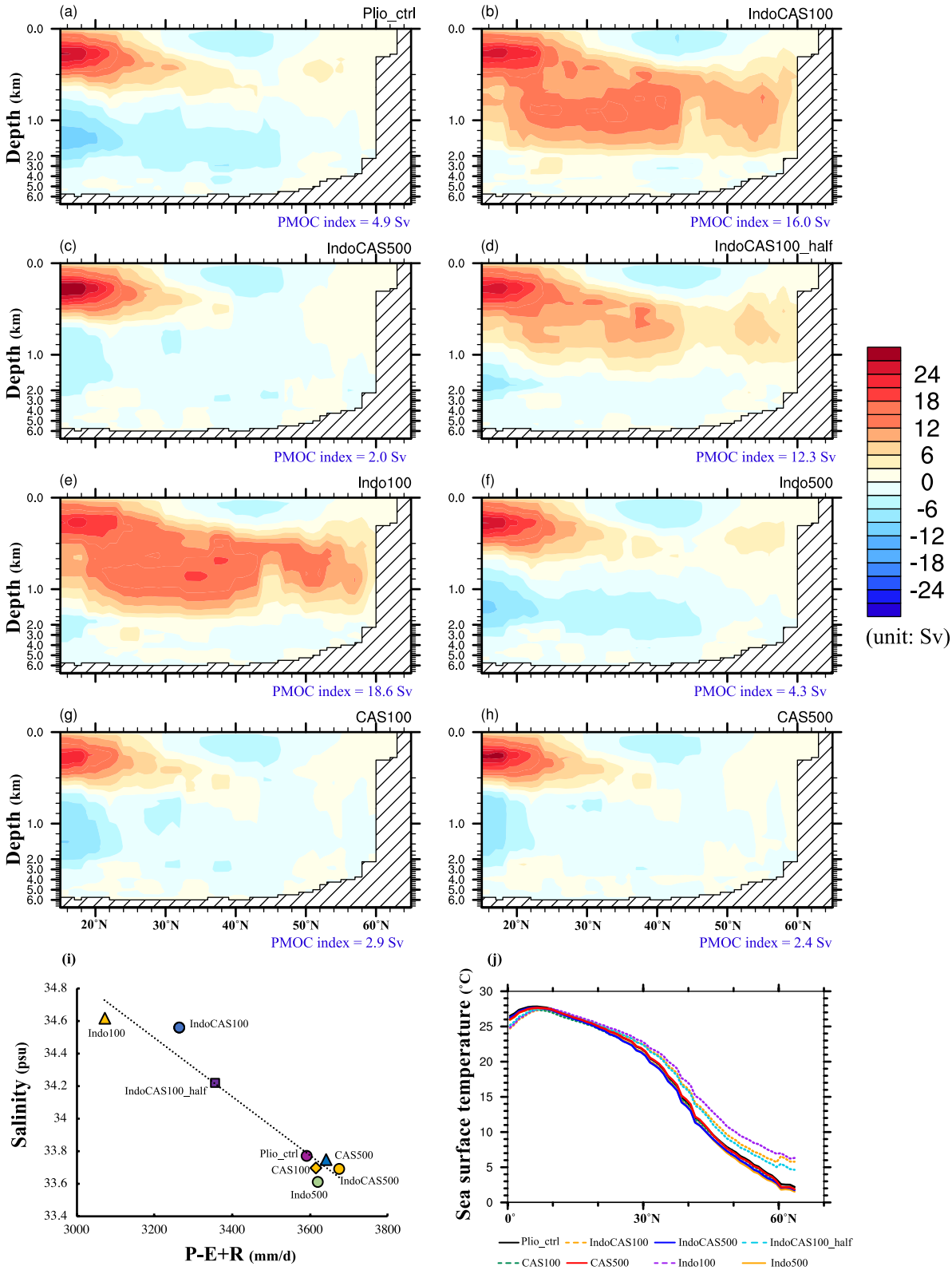

Figure 2. (a–h) Pacific meridional overturning circulation (PMOC) distribution over north of 15°N in (a) Plio_ctrl, (b) IndoCAS100, (c) IndoCAS500, (d) IndoCAS100_half, (e) Indo100, (f) Indo500, (g) CAS100, and (h) CAS500; (i) the relationship between mean annual total net precipitation (precipitation minus evaporation plus runoff) and mean annual surface salinity over subarctic Pacific region (40–65°N) in each experiment; (j) zonal mean sea surface temperatures in North Pacific in each experiment. PMOC index is defined as the maximum of the annual mean stream function below 500 m and over north of 25°N in the North Pacific.

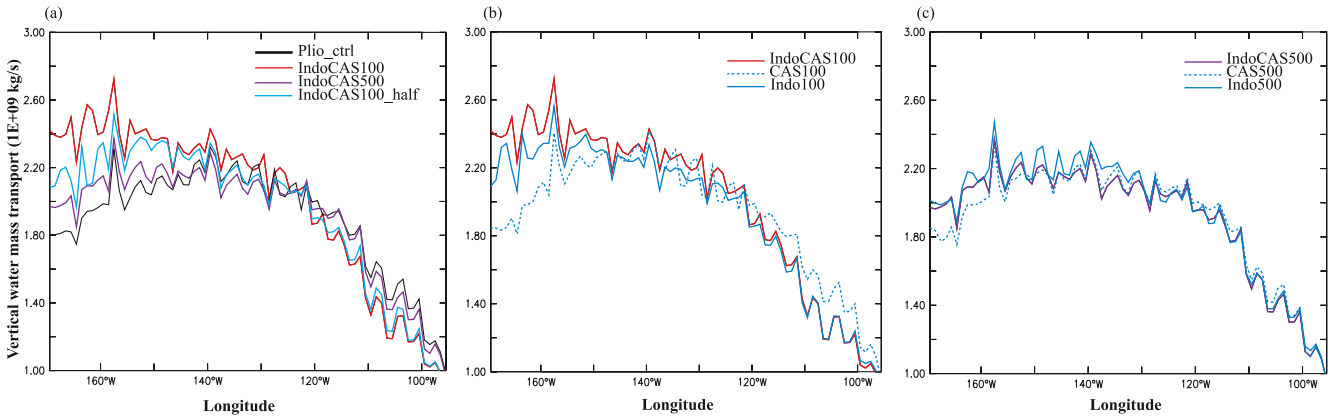

Figure 3. Upwelling strength at the Equator from the Central to Eastern Pacific (a) in Plio_ctrl and dual seaways experiments, (b) in IndoCAS100 and its related single seaway experiments, and (c) in IndoCAS500 and its related single seaway experiments. The upwelling strength is obtained with the maximum value of horizontally integrated vertical water flux (3°S–3°N) above the depth of 400 m.

Pacific in Plio_ctrl (Figure S5 in Supporting Information S1). When the tropical seaways (IndoCAS100 and IndoCAS100_half) are shallow and open, the easterly wind stress weakens in the east part of the EEP, but increases towards the CEP compared with Plio_ctrl. However, the wind stress changes very slightly along the equatorial region in IndoCAS500 relative to Plio_ctrl. These results are consistent with the related changes to the upwelling strengths.

4. Discussion

4.1. Comparison With Other Modeling Studies and Geological Records

As it is difficult to realistically constrain the timing and geometry of tropical seaways, we set two sill depths (100 and 500 m) and two widths for both CAS and Indonesian seaway in this study, which generally refer to the available reconstructions (Hall, 2002; Molnar & Cronin, 2015) across the late Miocene and early Pliocene. Compared with previous modeling studies, we notice spreads in simulations due to the different seaway geometry and applied models. Previous simulations with CESM (Brierley & Fedorov, 2016; Fedorov et al., 2013; Jochum et al., 2009) have shown the widening Indonesian seaway (by moving the northern tip of New Guinea south of the equator) has a weak impact on the global climate but can lead to reduction of the total ITF. However, studies based on KCM (Krebs et al., 2011; Song et al., 2017) have shown an increased total ITF, together with obvious impacts on the tropical Pacific SST and aridification in Australia owing to widening of the Indonesian seaway (by moving the northern tip of New Guinea and some land grids around Timor). In this study, we also observed increased ITF in the Indonesian seaway-only open experiment, which is more similar to the KCM work. Nevertheless, it is difficult to directly compare other features of the results between different modeling studies due to the different geometry settings of the seaways.

Supposing that IndoCAS500, IndoCAS100, and Plio_ctrl represent the scenarios for the Miocene, early Pliocene, and mid to late Pliocene, respectively, we notice that the simulated changes in zonal tropical Pacific SST gradient agree well with the reconstruction (Figure 4). We use the SST reconstructions from ocean drilling project (ODP) Site 806 in the western equatorial Pacific and from ODP Site 850 in the EEP to calculate the zonal gradients (Y. G. Zhang et al., 2014). We then take the simulated SST from the same location to calculate the simulated gradient. These data-model comparisons (Figure 4) show that the stepwise constriction of tropical seaways from deep to shallow and, finally, closure condition, produces similar change patterns in zonal SST gradient (4.3°C–3.5°C–4.4°C) to the reconstruction since the late Miocene (3.5°C–2.8°C–3.5°C). The relatively higher values of modeled zonal SST gradients are partly due to the model bias. The changes to the zonal SST gradients are coupling with changes to the meridional SST gradients (Figure 2j) in this work, that is consistent with previous study (Liu & Huang, 1997). Other evidence, such as the upper Miocene-Pliocene red clay deposits in the eastern Loess Plateau in China, show stronger aridity from ca. 6.2 to 5 Ma and weaker aridity from ca. 5 to ca. 3.6 Ma (Guo et al., 2004). These two stages may be partly associated with changes to the Pacific circulation

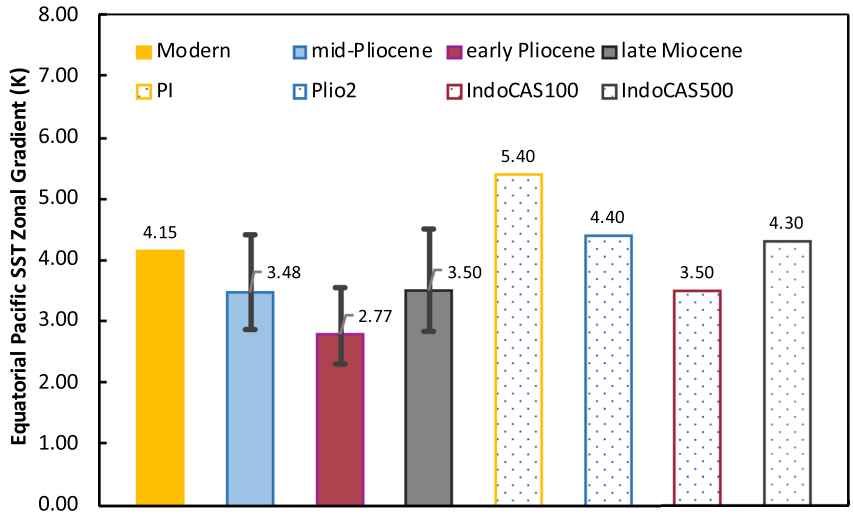

Figure 4. Equatorial Pacific sea surface temperature (SST) zonal gradients. Solid bars are the observed and reconstructed SST differences between WEP (ocean drilling project [ODP] 806) and EEP (ODP850). Modern data are from HadISST1 (Rayner et al., 2003) for the period of 1871–1890. Reconstructed data are derived from the TEX86 proxy, with the error bars indicating different calibration methods (Y. G. Zhang et al., 2014). In terms of different periods in this figure, the mid-Pliocene is defined as between 4 and 3 Ma, the early Pliocene between 5 and 4 Ma, and the late Miocene between 7 and 5 Ma. Dotted bars are modeling results calculated with the SSTs in the same locations as the ODP data (see ODP locations in Figure 1a).

as a result of the stepwise closure of seaways, which requires further attention in future work. Nevertheless, it should be noted that only changes of tropical seaways are considered in this study, but the climate during the late Miocene-Pliocene was affected by changes in many other factors; for example, insolation, GHGs, other tectonic factors, and other internal feedbacks.

4.2. Role of Tropical Seaways in the "Biogenic Bloom"

The biogenic bloom in the EEP during the late Miocene-Pliocene is well recorded in the $CaCO_3$ and bulk accumulation rate (Farrell et al., 1995; Schroeder et al., 1997), but the reasons for its development remain unclear. In fact, the reduced zonal SST gradient along the equatorial Pacific, as revealed from SST reconstructions (Wara et al., 2005; Y. G. Zhang et al., 2014), does not favor biological development, as the reduced gradient is usually linked to weakened wind-driven upwelling in modern understanding (Bjerknes, 1969), which is an important factor controlling the nutrient cycle in the surface system. Shankle et al. (2021) have invoked PMOC formation at that time to explain the reconstructed nutrient-enriched abyssal water supply in the EEP and to further reconcile the paradox of weaker upwelling and stronger productivity. There is indeed evidence of an active PMOC during that period in geological records (Burls et al., 2017). However, the active PMOC in the study of Shankle et al. (2021) is modeled by altering the cloud albedo gradients under which the reduced SST gradient can be established. Our study further suggests that a threshold of sill depth might exist for the impact of tropical seaways on the Pacific circulation. The active PMOC might be maintained by the shallow opening of tropical seaways (e.g., IndoCAS100 in this study). Nevertheless, it should be noted that favorable ocean dynamic conditions alone may not explain the whole story of the "biogenic bloom" during the late Miocene-Pliocene. The different-from-modern silicate and iron inputs (e.g., continuous tectonic activities in adjacent regions) should be also required for the biogenic bloom (Dugdale & Wilkerson, 1998).

5. Conclusions

In this study, we have investigated the impacts of the co-existence of the Indonesian seaway and CAS on the Pacific circulation for scenarios across the late Miocene-early Pliocene. Our results indicate that the sill depths of tropical seaways are critical for water mass transport through the seaways and further lead to different impacts

on the Pacific circulation and SST gradients. The shallow (100 m) opening of tropical seaways can trigger an active PMOC and enhance the Equatorial upwelling system, which can reduce both meridional and zonal SST gradients and help support a "biogenic bloom," whereas if both tropical seaways are deeper (subsurface depths, 500 m) there is a much weaker impact on the Pacific circulation. Single seaway experiments further show that the active PMOC can be attributed primarily to the shallow (100 m) widened Indonesian seaway, and the opening CAS has important influence on the ITF. Our results highlight the importance of the geometry of both tropical seaways. It is, however, worth noting that the model resolution in this study may to some extent make our results model-dependent. To exclude model dependency, future work should aim to use multi-models with identical geometry settings for seaways. Nevertheless, our study helps shed light on the importance of imposing strict geometric constraints on both tropical seaways in future work on this topic.

Data Availability Statement

The NorESM-L model description can be found in Bentsen et al. (2013) and Z. S. Zhang et al. (2012). Modelling data applied for the result analysis in this manuscript is deposited in the depository figshare with DOI: https://figshare.com/articles/dataset/NorESM-L_modeling_data_for_the_study_of_tropical_seaways/19800025. The SST reconstructed data is available through Y. G. Zhang et al. (2014). The modern SST data is available from HadISST1 data archive (https://www.metoffice.gov.uk/hadobs/hadisst/data/download.html, Rayner et al., 2003). Figures were plotted with the NCAR Command Language (version NCL 6.4.0; http://dx.doi.org/10.5065/D6WD3XH5) and Python version 2.7.15 (https://www.python.org/download/releases/2.7/).

Acknowledgments
This study was funded by the National Natural Science Foundation of China (NSFC programs 41888101 and 42125502). Ning Tan acknowledges support from the Strategic Priority Research Program of the Chinese Academy of Sciences (Grants XDB 26000000 andXDA13010106) and NSFC programs 41907371. Zhongshi Zhang acknowledges the SapienCE (Project 221712) from Norwegian Research Council. Zhilin He acknowledges NSFC programs 42007398. The authors thank Chunxia Zhang, Haibin Wu, Qinqzhen Hao, and Yongyun Hu for their helpful discussions. Many thanks to the editor and three reviewers (Anta-Clarisse Sarr, Chris Brierley, and one anonymous reviewer) for their constructive comments.

References

Auer, G., De Vleeschouwer, D., Smith, R. A., Bogus, K., Groeneveld, J., Grunert, P., et al. (2019). Timing and pacing of Indonesian throughflow restriction and its connection to Late Pliocene climate shifts. *Paleoceanography and Paleoclimatology*, *34*(4), 635–657. https://doi.org/10.1029/2018PA003512

Bentsen, M., Bethke, I., Debernard, J. B., Iversen, T., Kirkevåg, A., Seland, Ø., et al. (2013). The Norwegian Earth System Model, NorESM1-M–Part 1: Description and basic evaluation of the physical climate. *Geoscientific Model Development*, *6*(3), 687–720. https://doi.org/10.5194/gmd-6-687-2013

Bjerknes, J. (1969). Atmospheric teleconnections from the equatorial Pacific. *Monthly Weather Review*, *97*(3), 163–172. https://doi.org/10.1175/1520-0493(1969)097<0163:atftep>2.3.co;2

Bleck, R., Rooth, C., Hu, D., & Smith, L. T. (1992). Salinity-driven thermo. *Journal of Physical Oceanography*, *22*(12), 1486–1505. https://doi.org/10.1175/1520-0485(1992)022<1486:sdttia>2.0.co;2

Brierley, C. M., & Fedorov, A. V. (2016). Comparing the impacts of Miocene–Pliocene changes in inter-ocean gateways on climate: Central American Seaway, Bering Strait, and Indonesia. *Earth and Planetary Science Letters*, *444*, 116–130. https://doi.org/10.1016/j.epsl.2016.03.010

Burls, N. J., Fedorov, A. V., Sigman, D. M., Jaccard, S. L., Tiedemann, R., & Haug, G. H. (2017). Active Pacific meridional overturning circulation (PMOC) during the warm Pliocene. *Science Advances*, *3*(9), e1700156. https://doi.org/10.1126/sciadv.1700156

Cane, M. A., & Molnar, P. (2001). Closing of the Indonesian seaway as a precursor to east African aridification around 3 ± 4 million years ago. *Nature*, *411*(May), 157–162. https://doi.org/10.1038/35075500

Cerling, T. E., Harris, J. M., Macfadden, B. J., Leakey, M. G., Quade, J., Eisenmann, V., & Ehleringer, J. R. (1997). Global vegetation change through the Miocene/Pliocene boundary. *Nature*, *389*(6647), 153–158. https://doi.org/10.1038/38229

Christensen, B. A., Renema, W., Henderiks, J., De Vleeschouwer, D., Groeneveld, J., Castañeda, I. S., et al. (2017). Indonesian Throughflow drove Australian climate from humid Pliocene to arid Pleistocene. *Geophysical Research Letters*, *44*(13), 6914–6925. https://doi.org/10.1002/2017GL072977

Coates, A. G., & Stallard, R. F. (2013). How old is the Isthmus of Panama? *Bulletin of Marine Science*, *89*(4), 801–813. https://doi.org/10.5343/bms.2012.1076

Dowsett, H., Dolan, A., Rowley, D., Moucha, R., Forte, A. M., Mitrovica, J. X., et al. (2016). The PRISM4 (mid-Piacenzian) paleoenvironmental reconstruction. *Climate of the Past*, *12*(7), 1519–1538. https://doi.org/10.5194/cp-12-1519-2016

Driscoll, N. W., & Haug, G. H. (1998). A short circuit in thermohaline circulation: A cause for northern hemisphere glaciation? *Science*, *282*(5388), 436–438. https://doi.org/10.1126/science.282.5388.436

Drury, A. J., Liebrand, D., Westerhold, T., Beddow, H. M., Hodell, D. A., Rohlfs, N., et al. (2021). Climate, cryosphere and carbon cycle controls on Southeast Atlantic orbital-scale carbonate deposition since the Oligocene (30–0 Ma). *Climate of the Past*, *17*(5), 2091–2117. https://doi.org/10.5194/cp-17-2091-2021

Dugdale, R. C., & Wilkerson, F. (1998). Silicate regulation of new production in the equatorial Pacific upwelling Richard. *Nature*, *391*(January), 0–3. https://doi.org/10.1038/34630

Farrell, J. W., Raffi, I., Janecek, T. R., Murray, D. W., Levitan, M., Dadey, K. A., et al. (1995). 35. Late Neogene Sedimentation Patterns in the Eastern Equatorial Pacific Ocean. In N. G. Pisias, L. A. Mayer, T. R. Janecek, A. Palmer-Julson, & T. H. van Andel (Eds.), *Proceedings of the ocean drilling program, scientific results* (Vol. *138*).

Fedorov, A. V., Brierley, C. M., Lawrence, K. T., Liu, Z., Dekens, P. S., & Ravelo, A. C. (2013). Patterns and mechanisms of early Pliocene warmth. *Nature*, *496*(7443), 43–49. https://doi.org/10.1038/nature12003

Ferreira, D., Cessi, P., Coxall, H. K., De Boer, A., Dijkstra, H. A., Drijfhout, S. S., et al. (2018). Atlantic-Pacific asymmetry in deep water formation. *Annual Review of Earth and Planetary Sciences*, *46*(1), 327–352. https://doi.org/10.1146/annurev-earth-082517-010045

Ford, H. L., Burls, N. J., Jacobs, P., Jahn, A., Hodell, D. A., & Fedorov, A. V. (2022). Sustained mid-Pliocene warmth led to deep water formation in the North Pacific. *Nature Geoscience*, *15*(8), 658–663. https://doi.org/10.1038/s41561-022-00978-3

Gaina, C., & Müller, D. (2007). Cenozoic tectonic and depth/age evolution of the Indonesian gateway and associated back-arc basins. *Earth-Science Reviews*, *83*(3–4), 177–203. https://doi.org/10.1016/j.earscirev.2007.04.004

Guo, Z., Peng, S., Hao, Q., & Biscaye, P. E. (2004). Late Miocene– liocene development of Asian aridification as recorded in the Red-Earth Formation in northern China. *Global and Planetary Change*, *41*(3–4), 135–145. https://doi.org/10.1016/j.gloplacha.2004.01.002

Hall, R. (2002). Cenozoic geological and plate tectonic evolution of SE Asia and the SW Pacific: Computer-based reconstructions, model and animations. *Journal of Asian Earth Sciences*, *20*(4), 353–431. https://doi.org/10.1016/S1367-9120(01)00069-4

Haug, G. H., Tiedemann, R., Zahn, R., & Ravelo, A. (2001). Role of Panama uplift on oceanic freshwater balance. *Geology*, *851*(3), 207–210. https://doi.org/10.1130/0091-7613(2001)029<0207:ropuoo>2.0.co;2

Herbert, T. D., Lawrence, K. T., Tzanova, A., Peterson, L. C., Caballero-Gill, R., & Kelly, C. S. (2016). Late Miocene global cooling and the rise of modern ecosystems. *Nature Geoscience*, *9*(11), 843–847. https://doi.org/10.1038/ngeo2813

Huang, Y., Clemens, S. C., Liu, W., Wang, Y., & Prell, W. L. (2007). Large-scale hydrological change drove the late Miocene C4 plant expansion in the Himalayan foreland and Arabian Peninsula. *Geology*, *35*(6), 531–534. https://doi.org/10.1130/g23666a.1

Jansen, E., & Sjøholm, J. (1991). Reconstruction of glaciation over the past 6 Myr from ice-borne deposits in the Norwegian Sea. *Nature*, *349*(6310), 600–603. https://doi.org/10.1038/349600a0

Jochum, M., Fox-Kemper, B., Molnar, P. H., & Shields, C. (2009). Differences in the Indonesian seaway in a coupled climate model and their relevance to pliocene climate and El Niño. *Paleoceanography*, *24*(1), PA1212. https://doi.org/10.1029/2008PA001678

Karas, C., Nürnberg, D., Gupta, A. K., Tiedemann, R., Mohan, K., & Bickert, T. (2009). Mid-Pliocene climate change amplified by a switch in Indonesian subsurface Throughflow. *Nature Geoscience*, *2*(6), 434–438. https://doi.org/10.1038/ngeo520

Karatsolis, B.-T., Lougheed, B. C., De Vleeschouwer, D., & Henderiks, J. (2022). Abrupt conclusion of the late Miocene-early Pliocene biogenic bloom at 4.6–4.4 Ma. *Nature Communications*, *13*(1), 1–9. https://doi.org/10.1038/s41467-021-27784-6

Keigwin, L. (1982). Isotopic paleoceanography of the Caribbean and east Pacific: Role of Panama uplift in late Neogene time. *Science*, *217*(4557), 350–353. https://doi.org/10.1126/science.217.4557.350

Kessler, W. S. (2006). The circulation of the eastern tropical Pacific: A review. *Progress in Oceanography*, *69*(2–4), 181–217. https://doi.org/10.1016/j.pocean.2006.03.009

Krebs, U., Park, W., & Schneider, B. (2011). Pliocene aridification of Australia caused by tectonically induced weakening of the Indonesian throughflow. *Palaeogeography, Palaeoclimatology, Palaeoecology*, *309*(1–2), 111–117. https://doi.org/10.1016/j.palaeo.2011.06.002

Li, X., Guo, C., Zhang, Z., Helge Otterä, O., & Zhang, R. (2020). PlioMIP2 simulations with NorESM-L and NorESM1-F. *Climate of the Past*, *16*(1), 183–197. https://doi.org/10.5194/cp-16-183-2020

Liu, Z., & Huang, B. (1997). A coupled theory of tropical climatology: Warm pool, cold tongue, and Walker circulation. *Journal of Climate*, *10*(7), 1662–1679. https://doi.org/10.1175/1520-0442(1997)010<1662:actotc>2.0.co;2

Lunt, D. J., Foster, G. L., Haywood, A. M., & Stone, E. J. (2008). Late Pliocene Greenland glaciation controlled by a decline in atmospheric CO_2 levels. *Nature*, *454*(August), 1102–1105. https://doi.org/10.1038/nature07223

MaslinLi, M. X. S., Loutre, M. F., & Berger, A. (1998). The contribution of orbital forcing to the progressive intensification of Northern Hemisphere glaciation. *Quaternary Science Reviews*, *17*(97), 411–426. https://doi.org/10.1016/S0277-3791(97)00047-4

McCarthy, G. D., Smeed, D. A., Johns, W. E., Frajka-Williams, E., Moat, B. I., Rayner, D., et al. (2015). Measuring the Atlantic meridional overturning circulation at 26°N. *Progress in Oceanography*, *130*, 91–111. https://doi.org/10.1016/j.pocean.2014.10.006

Molnar, P., & Cronin, T. W. (2015). Growth of the maritime continent and its possible contribution to recurring ice ages. *Paleoceanography*, *30*(3), 196–225. https://doi.org/10.1002/2014PA002752

Montes, C., Cardona, A., Jaramillo, C., Pardo, A., Silva, J. C., Valencia, V., et al. (2015). Middle Miocene closure of the central American seaway. *Science*, *348*(6231), 226–229. https://doi.org/10.1126/science.aaa2815

Neale, R. B., Richter, J., Park, S., Lauritzen, P. H., Vavrus, S. J., Rasch, P. J., & Zhang, M. (2013). The mean climate of the community atmosphere model (CAM4) in forced SST and fully coupled experiments. *Journal of Climate*, *26*(14), 5150–5168. https://doi.org/10.1175/JCLI-D-12-00236.1

O'Dea, A., Lessios, H. A., Coates, A. G., Eytan, R. I., Restrepo-Moreno, S. A., Cione, A. L., et al. (2016). Formation of the Isthmus of Panama. *Science Advances*, *2*(8), 1–12. https://doi.org/10.1126/sciadv.1600883

Rayner, N. A. A., Parker, D. E., Horton, E. B., Folland, C. K., Alexander, L. V., Rowell, D. P., et al. (2003). Global analyses of sea surface temperature, sea ice, and night marine air temperature since the late nineteenth century. *Journal of Geophysical Research*, *108*(D14), 4407. https://doi.org/10.1029/2002jd002670

Rodgers, K. B., Latif, M., & Legutke, S. (2000). Sensitivity of equatorial Pacific and Indian Ocean watermasses to the position of the Indonesian throughflow. *Geophysical Research Letters*, *27*(18), 2941–2944. https://doi.org/10.1029/1999GL002372

Schroeder, J. O., Murray, R. W., Leinen, M., Pflaum, R. C., & Janecek, T. R. (1997). Barium in equatorial Pacific carbonate sediment: Terrigenous, oxide, and biogenic associations. *Paleoceanography*, *12*(1), 125–146. https://doi.org/10.1029/96PA02736

Shankle, M. G., Burls, N. J., Fedorov, A. V., Thomas, M. D., Liu, W., Penman, D. E., et al. (2021). Pliocene decoupling of equatorial Pacific temperature and pH gradients. *Nature*, *598*(7881), 457–461. https://doi.org/10.1038/s41586-021-03884-7

Song, Z., Latif, M., Park, W., Krebs-Kanzow, U., & Schneider, B. (2017). Influence of seaway changes during the pliocene on tropical Pacific climate in the Kiel climate model: Mean state, annual cycle, ENSO, and their interactions. *Climate Dynamics*, *48*(11–12), 3725–3740. https://doi.org/10.1007/s00382-016-3298-x

Sprintall, J., Wijffels, S. E., Molcard, R., & Jaya, I. (2009). Direct estimates of the Indonesian throughflow entering the Indian Ocean: 2004-2006. *Journal of Geophysical Research*, *114*(7), 2004–2006. https://doi.org/10.1029/2008JC005257

Thomas, M. D., Fedorov, A. V., Burls, N. J., & Liu, W. (2021). Oceanic pathways of an active Pacific meridional overturning circulation (PMOC). *Geophysical Research Letters*, *48*(10), 1–11. https://doi.org/10.1029/2020GL091935

Wara, M. W., Ravelo, A. C., & Delaney, M. L. (2005). Permanent El Nino-like conditions during the Pliocene warm period. *Science*, *309*(5735), 758–762. https://doi.org/10.1126/science.1112596

Zhang, Y. G., Pagani, M., & Liu, Z. (2014). A 12-million-year temperature history of the tropical Pacific ocean. *Science*, *344*(6179), 84–87. https://doi.org/10.1126/science.1246172

Zhang, Z. S., Nisancioglu, K., Bentsen, M., Tjiputra, J., Bethke, I., Yan, Q., et al. (2012). Pre-industrial and mid-Pliocene simulations with NorESM-L. *Geoscientific Model Development*, *5*(2), 523–533. https://doi.org/10.5194/gmd-5-523-2012